LETTERS

Mechanism of differential control of NMDA receptor activity by NR2 subunits

Marc Gielen[1], Beth Siegler Retchless[2], Laetitia Mony[1], Jon W. Johnson[2] & Pierre Paoletti[1]

***N*-methyl-D-aspartate (NMDA) receptors (NMDARs) are a major class of excitatory neurotransmitter receptors in the central nervous system. They form glutamate-gated ion channels that are highly permeable to calcium and mediate activity-dependent synaptic plasticity[1]. NMDAR dysfunction is implicated in multiple brain disorders, including stroke, chronic pain and schizophrenia[2]. NMDARs exist as multiple subtypes with distinct pharmacological and biophysical properties that are largely determined by the type of NR2 subunit (NR2A to NR2D) incorporated in the heteromeric NR1/NR2 complex[1,3,4]. A fundamental difference between NMDAR subtypes is their channel maximal open probability (P_o), which spans a 50-fold range from about 0.5 for NR2A-containing receptors to about 0.01 for receptors containing NR2C and NR2D; NR2B-containing receptors have an intermediate value (about 0.1)[5–9]. These differences in P_o confer unique charge transfer capacities and signalling properties on each receptor subtype[4,6,10,11]. The molecular basis for this profound difference in activity between NMDAR subtypes is unknown. Here we show that the subunit-specific gating of NMDARs is controlled by the region formed by the NR2 amino-terminal domain (NTD), an extracellular clamshell-like domain previously shown to bind allosteric inhibitors[12–15], and the short linker connecting the NTD to the agonist-binding domain (ABD). The subtype specificity of NMDAR P_o largely reflects differences in the spontaneous (ligand-independent) equilibrium between open-cleft and closed-cleft conformations of the NR2-NTD. This NTD-driven gating control also affects pharmacological properties by setting the sensitivity to the endogenous inhibitors zinc and protons. Our results provide a proof of concept for a drug-based bidirectional control of NMDAR activity by using molecules acting either as NR2-NTD 'closers' or 'openers' promoting receptor inhibition or potentiation, respectively.**

We first explored the role of the NR2-NTD in the difference of P_o between NR1/NR2A and NR1/NR2B receptors by evaluating the effect of deleting the entire NR2-NTD on receptor activity. We estimated P_o by using a method based on the covalent modification of a cysteine residue introduced in the NR1 subunit (NR1-A652C), which locks open the NMDAR channel[16]. Although this method does not give access to the absolute P_o of receptors containing the wild-type NR1 (NR1wt) subunit, it can report relative differences in channel activity[17]. Indeed, the extent to which the thiol-modifying reagent 2-aminoethylmethanethiosulphonatehydrobromide (MTSEA) potentiates NMDAR currents is inversely related to the channel P_o (ref. 17). MTSEA potentiated currents carried by NR1-A652C/NR2B receptors to a much greater extent than currents of NR1-A652C/NR2A receptors (Fig. 1a, d), consistent with the much lower P_o of NR2B-containing receptors than that of NR2A-containing receptors[5,6,17]. In contrast, MTSEA-induced potentiations of NR1-A652C/NR2A-ΔNTD and NR1-A652C/NR2B-ΔNTD receptors were indistinguishable (Fig. 1b, d), indicating equal receptor activities. However, receptors incorporating chimaeric NR2A-(2B NTD) or NR2B-(2A NTD) subunits displayed MTSEA-induced potentiations similar to those of the parental NR2 subunits, indicating that swapping the NTDs alone did not exchange the P_o (Fig. 1d). We therefore swapped both the NTD and the highly divergent short (14 residues) linker segment that connects the NTD to the ABD (Supplementary Fig. 1). NR1-A652C/NR2A-(2B NTD+L) and NR1-A652C/NR2B-(2A NTD+L) responses supported levels of MTSEA potentiation closer to those of NR2Bwt-containing and NR2Awt-containing receptors, respectively (Fig. 1c, d). Direct measurement of channel activity with single-channel recordings confirmed this exchange of P_o (Fig. 1e and Supplementary Fig. 2).

We next extended the analysis to the NR2D subunit. MTSEA-induced potentiations of NR2D-containing receptors were considerable (about 300-fold), reflecting the very low P_o of NR1/NR2D receptors (Fig. 1d). Deleting the NR2D-NTD resulted in a fourfold decrease in MTSEA potentiation, indicative of a markedly increased P_o (Fig. 1d). This gain-of-function phenotype could be reinforced by grafting onto NR2D-ΔNTD the NTD plus linker (NTD+L) region of the high-P_o subunit NR2A. Conversely, receptors containing the chimaeric NR2A-(2D NTD+L) subunit displayed 17-fold higher potentiation by MTSEA than NR2Awt-containing receptors, suggestive of a much lower P_o (Fig. 1d). Thus, the low P_o of the NR2D-containing receptors is also set by the NR2-NTD.

Because the estimation of P_o with MTSEA relies on a mutated NR1 subunit (NR1-A652C), we checked that the effects observed did not depend on this mutation. We used the time constant of inhibition by MK-801, an NMDAR open-channel blocker, as an alternative method of assessing P_o (refs 5, 18). Consistent with the higher P_o of receptors containing NR2A than that of receptors containing NR2B, MK-801 inhibited wild-type NR1/NR2A receptors significantly faster than wild-type NR1/NR2B receptors (Supplementary Fig. 3a, b). Deleting the NR2-NTDs abolished this difference (Supplementary Fig. 3b). Whereas swapping the NR2-NTD alone did not exchange MK-801 time constants, incorporating the NTD-ABD linker achieved almost complete transfer (Supplementary Fig. 3a, b). As expected, the onset of MK-801 inhibition at wild-type NR1/NR2D receptors was much slower than that at receptors containing NR2A or NR2B. Deleting the NR2D-NTD or replacing the NTD+L region of NR2D by that of NR2A strongly accelerated MK-801 inhibition, indicative of a much increased P_o (Fig. 1f and Supplementary Fig. 3c). Conversely, MK-801 inhibition of receptors incorporating NR2A-(2D NTD+L) was 15-fold slower than at NR2Awt-containing receptors (Supplementary Fig. 3b). Together with the MTSEA experiments, these results demonstrate that the NR2-NTD+L region is a major determinant of the NR2 subunit-specific activity of NMDARs.

[1]Laboratoire de Neurobiologie, École Normale Supérieure, CNRS, 46 rue d'Ulm, 75005 Paris, France. [2]Department of Neuroscience, University of Pittsburgh, A210 Langely Hall, Pittsburgh, Pennsylvania 15260, USA.

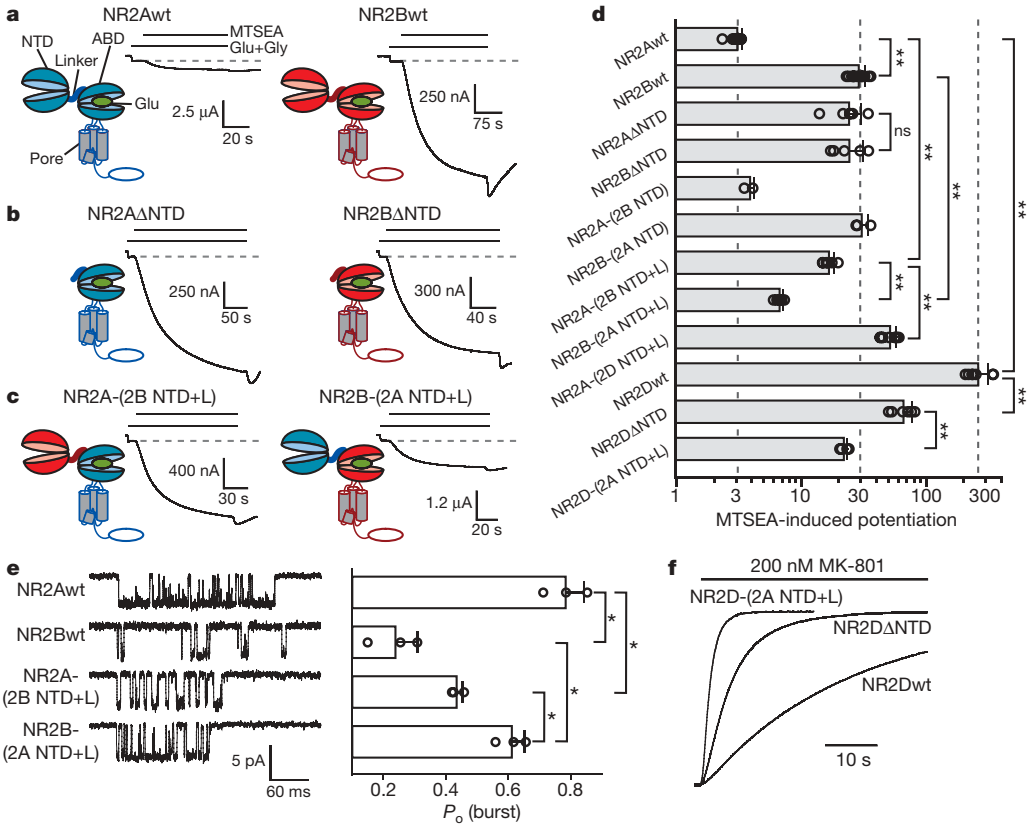

Figure 1 | The NR2 NTD+L region controls NMDAR P_o. **a–c**, Potentiation by MTSEA of receptors incorporating NR1-A652C and NR2Awt or NR2Bwt (**a**), NR2A-ΔNTD or NR2B-ΔNTD (**b**), and NR2A-(2B NTD+L) or NR2B-(2A NTD+L) (**c**). **d**, Pooled data (means ± s.d.), from top to bottom: 3.2 ± 0.3 ($n = 12$), 30 ± 4 ($n = 14$), 25 ± 6 ($n = 6$), 25 ± 7 ($n = 5$), 4.0 ± 0.3 ($n = 3$), 32 ± 4 ($n = 3$), 17 ± 2 ($n = 6$), 6.9 ± 0.5 ($n = 5$), 53 ± 7 ($n = 9$), 270 ± 60 ($n = 7$), 68 ± 12 ($n = 6$) and 23 ± 2 ($n = 5$). Two asterisks, $P < 0.001$. **e**, P_o within bursts of openings for receptors incorporating NR1wt and the indicated NR2 subunit. Left: representative traces of bursts. Right (from top to bottom): 0.78 ± 0.06 ($n = 3$), 0.24 ± 0.07 ($n = 3$), 0.43 ± 0.02 ($n = 3$) and 0.61 ± 0.04 ($n = 3$). Asterisk, $P < 0.05$, Student's *t*-test. Error bars represent s.d. **f**, Kinetics of inhibition by 200 nM MK-801 at receptors incorporating NR1wt and NR2Dwt ($\tau_{on} = 32$ s), NR2D-ΔNTD (5.7 s) or NR2D-(2A NTD+L) (1.6 s).

We then investigated the mechanism by which a distal domain, the NR2-NTD, influences channel activity. Previous studies on allosteric inhibition of NMDARs by NR2-NTD ligands, such as zinc and ifenprodil, suggested that these ligands bind the NTD cleft and promote its closure[12,15,19]. This in turn leads to receptor inhibition through disruption of the NR1/NR2 ABD dimer interface, resembling

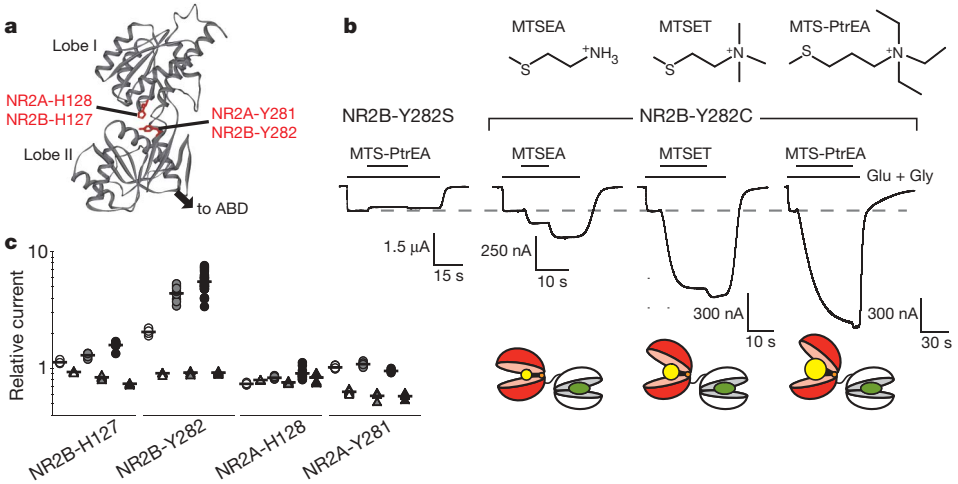

Figure 2 | Locking open the NR2-NTD increases NMDAR activity. **a**, Three-dimensional model of NR2B-NTD. **b**, Top: chemical formula of the transferable moiety of MTSEA, MTSET and MTS-PtrEA. Middle: recordings from NR1wt/NR2B-Y282C and control NR1wt/NR2B-Y282S receptors during treatment with MTS. The potentiation after washout of MTS probably reflects the washout of a reversible pore-blocking effect of the positively charged MTS. Bottom: schematic representations of the NTD-ABD tandem of NR2B-Y282C after modification by MTS (MTS headgroup in yellow). **c**, Relative currents after application of MTSEA (white symbols), MTSET (grey symbols) and MTS-PtrEA (black symbols) to receptors incorporating NR1wt and the indicated NR2 subunit harbouring a cysteine mutation (circles) or a control mutation (triangles). See Supplementary Table 1 for values.

the mechanism underlying the desensitization of AMPA (α-amino-3-hydroxy-5-methyl-4-isoxazole propionic acid) receptors[20–22]. Because the NTD can adopt at least two conformations, a ligand-free open state and a ligand-bound closed state, we speculated that the NTD-driven control of P_o might result from spontaneous oscillations of the NR2-NTD between an open-cleft conformation, favouring channel opening, and a closed-cleft conformation, favouring pore closure. Similar ligand-independent oscillations have been observed in several clamshell-like proteins, including the bacterial maltose-binding protein[23] (MBP) and the $GABA_B$ (γ-aminobutyric acid B) receptor[24]. To test this hypothesis, we introduced cysteine residues into the NR2-NTD cleft to lock open the NR2-NTDs with the use of thiol-reactive methanethiosulphonate (MTS) reagents. On the basis of three-dimensional models, we first introduced a cysteine residue deep in the cleft of the NR2B-NTD by mutating the hinge residue NR2B-Y282, whose side chain points towards the cleft entrance[25] (Fig. 2a). Application of the positively charged MTSEA potentiated NR1wt/NR2B-Y282C receptors but not control NR1wt/NR2B-Y282S receptors (Fig. 2b). Using MTS compounds of the same valence but different sizes (2-[trimethylammonium]ethylmethanethiosulphonatebromide [MTSET] and 3-[triethylammonium]propylmethanethiosulphonatebromide [MTS-PtrEA]), we observed that the potentiation increased with increasing MTS size (Fig. 2b, c). Comparison of the rates of inhibition by MK-801 before and after treatment with MTS, together with direct measurement of single-channel activity, revealed that current potentiations reflected an increase in P_o (Supplementary Figs 4 and 5). Sensitivity to glycine (binding the NR1-ABD) was unaltered by treatment with MTS, whereas sensitivity to glutamate (binding the NR2-ABD) was slightly decreased (Supplementary Fig. 6), as expected from the known allosteric interaction between the NR2 NTD and ABD[26]. MTS action was significantly faster on resting receptors than on activated receptors (Supplementary Fig. 7), further arguing for a facilitated opening of the NR2-NTD when the ABD is open. Taken together, these results show that trapping open the NR2-NTD enhances receptor activity. They also indicate that the NTD of NR2B-Y282C is neither permanently open (because there was a potentiating effect of the MTS compounds) nor closed (because the introduced cysteine residue was accessible to MTS), but rather alternates between open and closed conformations, the latter favouring pore closure.

Because NR2B-Y282 is a large residue, we considered the possibility that its mutation into a small residue (cysteine or serine) might have artificially increased the flexibility of the NTD hinge, favouring NTD closure. Indeed, such mutations strongly decreased receptor activity (Supplementary Fig. 8). This effect highlights the unsuspected role of the NR2-NTD hinge in shaping NMDAR P_o, reminiscent of the critical role of the MBP hinge in controlling the apparent maltose affinity[27]. To extend our conclusion of spontaneous NR2-NTD oscillations to receptors with unaltered gating properties, we targeted H127 of NR2B-NTD, because its mutation into cysteine minimally affects receptor activity (Supplementary Fig. 8). MTS compounds still potentiated NR1wt/NR2B-H127C receptors (but not control NR1wt/NR2B-H127A receptors) in a size-dependent manner. However, potentiations were considerably smaller than with NR1wt/NR2B-Y282C receptors (Fig. 2c and Supplementary Fig. 9a). Two reasons may explain this difference: higher basal P_o of NR1wt/NR2B-H127C receptors, and wider opening of the NTD at MTS-modified NR2B-Y282C subunits because of the deeper location of Y282 in the cleft. Taken together, these results provide the new information that spontaneous oscillations of the NR2B-NTD contribute to the low P_o of wild-type NR1/NR2B receptors.

We then tested the prediction that the high P_o of NR2A-containing receptors results from the preference of NR2A-NTD for the open conformation. As with NR2B, we found the P_o of NR2A-containing receptors to be significantly decreased by the mutation of NR2A-Y281 into small residues (Supplementary Fig. 8). A potentiating component was also observed at receptors containing NR2A-Y281C during treatment with MTS compounds, but not at control NR2A-Y281A receptors. However, MTS-induced potentiations were much smaller than at NR2B-Y282C receptors and were independent of MTS size (Fig. 2c and Supplementary Fig. 9b), suggesting that the NR2A-NTD is much less sensitive to steric hindrance than the NR2B-NTD. In addition, no potentiation was observed at NR2A-H128C receptors even with the larger MTSET and MTS-PtrEA (Fig. 2c and Supplementary Fig. 9b). This is consistent with the idea that NR2A-NTD spends most of its time in an open-cleft conformation, thus contributing to the relatively high P_o of NR2A-containing receptors.

Our results on chimaeric NR2 subunits, showing that the NTD-ABD linker is required for the differential influence of the NR2-NTD on receptor P_o, raised the possibility that this element is also crucial during the allosteric modulation of NMDARs by NTD ligands. NR2A-NTD forms a high-affinity zinc inhibitory site[12–14]; in accord with this, NR1wt/NR2D-(2A NTD+L) receptors were highly sensitive to zinc (Fig. 3a). NR1wt/NR2B-(2A NTD) receptors are also highly sensitive to zinc. Surprisingly, zinc is much more potent at these receptors than at wild-type NR1/NR2A receptors (Fig. 3a), suggesting that the NR2B NTD-ABD linker facilitates NTD-cleft closure. Increasing the chimaera length to incorporate the NR2A NTD-ABD linker almost completely restored NR2Awt-like zinc sensitivity (Fig. 3a). This again highlights the importance of the

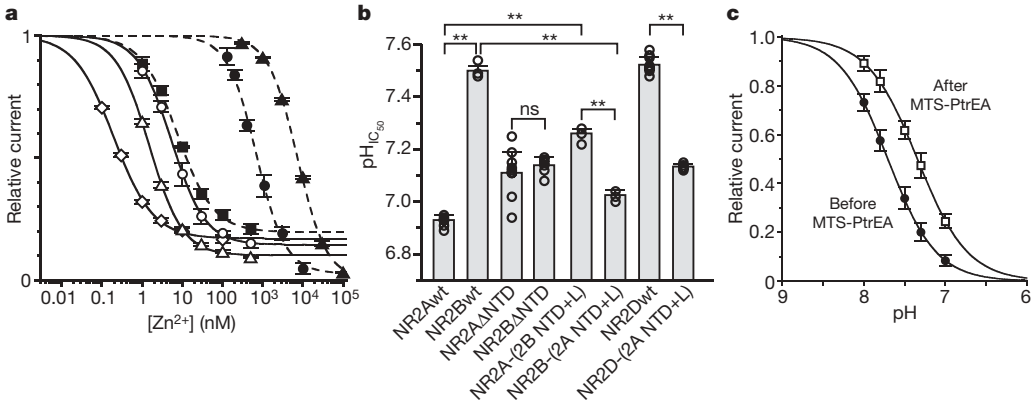

Figure 3 | The NR2 NTD+L region controls zinc and proton sensitivities of NMDARs. **a**, Zinc sensitivity of receptors incorporating NR1wt and NR2Awt (filled squares; maximum inhibition 81%, IC_{50} 7.5 nM; $n = 6$), NR2Bwt (filled circles; 98%, 720 nM; $n = 13$), NR2Dwt (filled triangles; 100%, 7.8 μM; $n = 3$), NR2B-(2A NTD) (open diamonds; 83%, 0.20 nM; $n = 4$), NR2B-(2A NTD+L) (open circles; 86%, 5.4 nM; $n = 4$) or NR2D-(2A NTD+L) (open triangles; 90%, 1.5 nM; $n = 5$). n_H was in the range 0.9–1.2. **b**, $pH_{IC_{50}}$ of receptors incorporating NR1wt and the indicated NR2 subunits. See Supplementary Table 2 for values. Two asterisks, $P < 0.001$. **c**, Proton sensitivity of NR1wt/NR2B-Y282C receptors before ($pH_{IC_{50}} = 7.70$, $n_H = 1.5$; $n = 3$) and after ($pH_{IC_{50}} = 7.34$, $n_H = 1.4$; $n = 3$) modification by MTS-PtrEA. Error bars represent s.d.

NTD-ABD linker for communication between the NTD and the gating machinery.

Protons are another allosteric modulator that differentially inhibit NMDAR subtypes[1]. In contrast with the zinc sensor, the proton sensor is thought to be closely associated with the channel gate[28]. Unexpectedly, deleting the NR2-NTDs fully abolished the difference in pH sensitivity between wild-type NR1/NR2A and NR1/NR2B receptors (Fig. 3b). Moreover, swapping the NTD+L region between NR2A and NR2B reversed their pH sensitivities, whereas grafting the NR2A NTD+L region onto NR2D decreased its proton sensitivity towards that of NR2Awt-containing receptors (Fig. 3b). Proton sensitivity was also decreased when the NR2B-Y282C NTD was locked open with MTS-PtrEA (Fig. 3c). Therefore the NR2 dependence of pH sensitivity is unlikely to result from an intrinsic difference in the proton sensor between NR1/NR2 receptor subtypes, but rather from differential access to the proton-binding site owing to the influence of NR2-NTD on channel activity.

Our study reveals that the large differences in channel activity conferred by the various NR2 NMDAR subunits originate from a region remote from the agonist-binding/channel gating core. This region comprises the large NR2-NTD and the short linker connecting the NR2-NTD to the ABD. The bilobate NR2-NTD oscillates spontaneously between open-cleft and closed-cleft conformations (Fig. 4), the latter triggering disruption of the ABD dimer interface and subsequent channel closure[20]. The NTD-ABD linker could exert its key influence by tuning the equilibrium between the different conformations of the NR2-NTD. The identity of the NR2-NTD+L region also determines the sensitivity to zinc and protons, two endogenous allosteric inhibitors of NMDARs that are likely to be critical in the regulation of NMDAR activity under physiological and pathological conditions[1,3]. Through its dynamic conformational equilibrium, the NR2-NTD could serve as a target for either negative or positive subunit-specific allosteric modulators (Fig. 4). Compounds such as ifenprodil, which bind the NTD cleft and promote its closure (NTD 'closers'), behave as subunit-specific NMDAR inhibitors and show good efficacy as neuroprotectants[2]. We propose that molecules that bind the same cleft but impede its closure (NTD 'openers') would behave as NMDAR potentiators (Fig. 4). Such molecules may prove to be of significant therapeutic benefit, given the accumulating evidence that major human psychoses, including schizophrenia, are associated with a deficit of NMDAR activity[2,29].

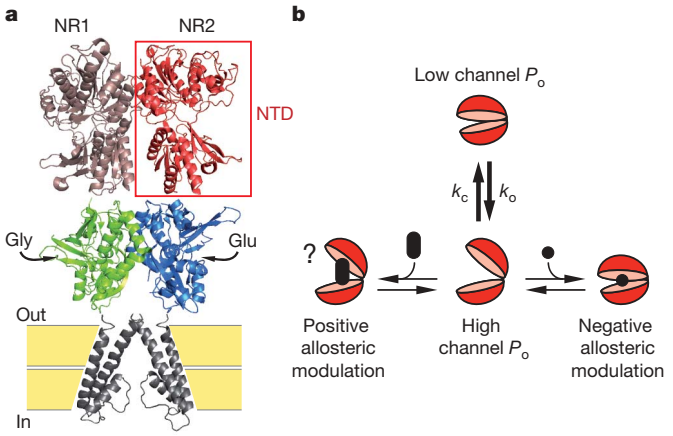

Figure 4 | Model for the control of NMDAR activity by the N-terminal domain of NR2. a, Structural depiction of an NMDAR. The full receptor is a tetramer, but only an NR1/NR2 dimer is shown[30]. **b**, In its ligand-free state, the NR2-NTD alternates between open-cleft and closed-cleft conformations, the latter favouring pore closure. In the model, this equilibrium determines the subtype specificity of NMDAR P_o; k_o/k_c(NR2B) < k_o/k_c(NR2A). The NTD is also the target of subunit-specific allosteric inhibitors such as zinc[12–14,19] or ifenprodil[15,25], which bind the central cleft of the NTD and promote domain closure. We propose that a molecule binding in the same cleft, but preventing its closure, behaves as a positive allosteric modulator, enhancing receptor activity.

METHODS SUMMARY

Complementary DNA constructs and site-directed mutagenesis. The pcDNA3-based expression plasmids, mutagenesis and sequencing procedure have been described previously[19]. Chimaeras were obtained by classical amplification by polymerase chain reaction and subsequent subcloning into the parental clone.

Electrophysiology. Recombinant NMDARs were expressed in *Xenopus laevis* oocytes after simultaneous injection of cDNAs (at 10 ng μl^{-1}; nuclear injection) coding for the various NR1 and NR2 subunits (ratio 1:1). Oocytes were prepared, injected, voltage-clamped and superfused as described previously[12].

Single channels were recorded from human embryonic kidney (HEK)-cell outside-out patches.

Full Methods and any associated references are available in the online version of the paper at www.nature.com/nature.

Received 1 December 2008; accepted 16 March 2009.
Published online 29 April 2009.

1. Dingledine, R., Borges, K., Bowie, D. & Traynelis, S. F. The glutamate receptor ion channels. *Pharmacol. Rev.* **51,** 7–61 (1999).
2. Kemp, J. A. & McKernan, R. M. NMDA receptor pathways as drug targets. *Nature Neurosci.* **5** (Suppl.), 1039–1042 (2002).
3. Paoletti, P. & Neyton, J. NMDA receptor subunits: function and pharmacology. *Curr. Opin. Pharmacol.* **7,** 39–47 (2007).
4. Cull-Candy, S. G. & Leszkiewicz, D. N. Role of distinct NMDA receptor subtypes at central synapses. *Sci. STKE* **2004,** re16 (2004).
5. Chen, N., Luo, T. & Raymond, L. A. Subtype-dependence of NMDA receptor channel open probability. *J. Neurosci.* **19,** 6844–6854 (1999).
6. Erreger, K., Dravid, S. M., Banke, T. G., Wyllie, D. J. & Traynelis, S. F. Subunit-specific gating controls rat NR1/NR2A and NR1/NR2B NMDA channel kinetics and synaptic signalling profiles. *J. Physiol. (Lond.)* **563,** 345–358 (2005).
7. Wyllie, D. J., Behe, P. & Colquhoun, D. Single-channel activations and concentration jumps: comparison of recombinant NR1a/NR2A and NR1a/NR2D NMDA receptors. *J. Physiol. (Lond.)* **510,** 1–18 (1998).
8. Dravid, S. M., Prakash, A. & Traynelis, S. F. Activation of recombinant NR1/NR2C NMDA receptors. *J. Physiol. (Lond.)* **586,** 4425–4439 (2008).
9. Popescu, G., Robert, A., Howe, J. R. & Auerbach, A. Reaction mechanism determines NMDA receptor response to repetitive stimulation. *Nature* **430,** 790–793 (2004).
10. Liu, Y. *et al.* NMDA receptor subunits have differential roles in mediating excitotoxic neuronal death both *in vitro* and *in vivo*. *J. Neurosci.* **27,** 2846–2857 (2007).
11. Liu, L. *et al.* Role of NMDA receptor subtypes in governing the direction of hippocampal synaptic plasticity. *Science* **304,** 1021–1024 (2004).
12. Paoletti, P. *et al.* Molecular organization of a zinc binding N-terminal modulatory domain in a NMDA receptor subunit. *Neuron* **28,** 911–925 (2000).
13. Low, C. M., Zheng, F., Lyuboslavsky, P. & Traynelis, S. F. Molecular determinants of coordinated proton and zinc inhibition of *N*-methyl-D-aspartate NR1/NR2A receptors. *Proc. Natl Acad. Sci. USA* **97,** 11062–11067 (2000).
14. Choi, Y. B. & Lipton, S. A. Identification and mechanism of action of two histidine residues underlying high-affinity Zn^{2+} inhibition of the NMDA receptor. *Neuron* **23,** 171–180 (1999).
15. Perin-Dureau, F., Rachline, J., Neyton, J. & Paoletti, P. Mapping the binding site of the neuroprotectant ifenprodil on NMDA receptors. *J. Neurosci.* **22,** 5955–5965 (2002).
16. Jones, K. S., VanDongen, H. M. & VanDongen, A. M. The NMDA receptor M3 segment is a conserved transduction element coupling ligand binding to channel opening. *J. Neurosci.* **22,** 2044–2053 (2002).
17. Yuan, H., Erreger, K., Dravid, S. M. & Traynelis, S. F. Conserved structural and functional control of *N*-methyl-D-aspartate receptor gating by transmembrane domain M3. *J. Biol. Chem.* **280,** 29708–29716 (2005).
18. Blanke, M. L. & VanDongen, A. M. Constitutive activation of the *N*-methyl-D-aspartate receptor via cleft-spanning disulfide bonds. *J. Biol. Chem.* **283,** 21519–21529 (2008).
19. Rachline, J., Perin-Dureau, F., Le Goff, A., Neyton, J. & Paoletti, P. The micromolar zinc-binding domain on the NMDA receptor subunit NR2B. *J. Neurosci.* **25,** 308–317 (2005).
20. Gielen, M. *et al.* Structural rearrangements of NR1/NR2A NMDA receptors during allosteric inhibition. *Neuron* **57,** 80–93 (2008).
21. Sun, Y. *et al.* Mechanism of glutamate receptor desensitization. *Nature* **417,** 245–253 (2002).
22. Mayer, M. L. Glutamate receptors at atomic resolution. *Nature* **440,** 456–462 (2006).
23. Tang, C., Schwieters, C. D. & Clore, G. M. Open-to-closed transition in apo maltose-binding protein observed by paramagnetic NMR. *Nature* **449,** 1078–1082 (2007).

24. Kniazeff, J. *et al.* Locking the dimeric $GABA_B$ G-protein-coupled receptor in its active state. *J. Neurosci.* **24,** 370–377 (2004).
25. Mony, L. *et al.* Structural basis of NR2B-selective antagonist recognition by *N*-methyl-D-aspartate receptors. *Mol. Pharmacol.* **75,** 60–74 (2009).
26. Zheng, F. *et al.* Allosteric interaction between the amino terminal domain and the ligand binding domain of NR2A. *Nature Neurosci.* **4,** 894–901 (2001).
27. Marvin, J. S. & Hellinga, H. W. Manipulation of ligand binding affinity by exploitation of conformational coupling. *Nature Struct. Biol.* **8,** 795–798 (2001).
28. Low, C. M. *et al.* Molecular determinants of proton-sensitive *N*-methyl-D-aspartate receptor gating. *Mol. Pharmacol.* **63,** 1212–1222 (2003).
29. Lisman, J. E. *et al.* Circuit-based framework for understanding neurotransmitter and risk gene interactions in schizophrenia. *Trends Neurosci.* **31,** 234–242 (2008).
30. Furukawa, H., Singh, S. K., Mancusso, R. & Gouaux, E. Subunit arrangement and function in NMDA receptors. *Nature* **438,** 185–192 (2005).

Supplementary Information is linked to the online version of the paper at www.nature.com/nature.

Acknowledgements We thank B. Barbour, P.-J. Corringer, J. Neyton and D. Stroebel for comments on the manuscript, and S. Carvalho, M. Casado and M. Gendrel for experimental help. This work was supported by the Ministère de la Recherche (M.G., L.M.), the Université Pierre et Marie Curie (UPMC) and the Fondation pour la Recherche Médicale (FRM) (M.G.), NIH grant R01 MH045817 (J.W.J.), the Institut National de la Santé et de la Recherche Médicale (INSERM), the Agence Nationale pour la Recherche (ANR), GlaxoSmithKline and an Équipe FRM grant (P.P.).

Author Information Reprints and permissions information is available at www.nature.com/reprints. Correspondence and requests for materials should be addressed to P.P. (paoletti@biologie.ens.fr).

METHODS

Two electrode voltage-clamp recordings and analysis. For all experiments, except those aimed at measuring pH sensitivity, the standard external solution contained (in mM): 100 NaCl, 2.5 KCl, 0.3 $BaCl_2$, 5 HEPES; pH adjusted to 7.3 with NaOH. To chelate trace amounts of contaminant zinc, diethylenetriaminepentaacetic acid (DTPA) (10 μM) was added to all the '0' zinc solutions[31]. For free zinc concentrations in the range 1 nM–1 μM, tricine (10 mM) was used to buffer zinc, whereas *N*-[2-acetamido]-iminodiacetic acid (ADA) (1 mM) was used to buffer zinc in the 0.1–100 nM range[20]. For the pH sensitivity experiments, an enriched HEPES external solution was used to ensure proper pH buffering[20]. Currents were elicited by the simultaneous application of saturating concentrations of glutamate and glycine (100 μM each), and measured at a holding potential of −60 mV. MTS compounds were used at 0.2 mM (except in Supplementary Fig. 7). Experiments were performed at room temperature (18–25 °C). Data collection and analysis of pH and zinc dose–response curves were performed as described in ref. 20. MK-801 time constants of inhibition were obtained by fitting currents with a single-exponential component within a time window corresponding to 10–90% of the maximal inhibition. Data points used for statistical tests were assumed log-normally distributed before performing a Student's *t*-test (unless otherwise indicated).

Single-channel recordings and analysis. HEK cells were transfected with 2 μg of cDNAs mixed in a ratio of 1 NR1:3 NR2:3 green fluorescent protein (GFP), using calcium phosphate precipitation or FuGENE Transfection Reagent (Roche). Positive cells were revealed by GFP epifluorescence. Patch pipettes of 5–10 MΩ were filled with a solution containing (in mM): 115 CsF, 10 CsCl, 10 HEPES, 10 EGTA; pH adjusted to 7.15 with CsOH. The osmolality was 270 mosmol kg^{-1}. The standard external solution contained (in mM): 140 NaCl, 2.8 KCl, 0.5 $CaCl_2$, 10 HEPES, 0.01 EDTA; pH adjusted to 7.3 with NaOH. Osmolality was adjusted to 290 mosmol kg^{-1} with sucrose. EDTA was added to chelate trace amounts of contaminant zinc[31]. Channel openings were activated by 100 μM glycine, with 0.05 or 0.01 μM glutamate in most experiments, or with 100 μM glutamate in some patches (included only if no double openings were observed). The holding potential (after correction for junction potential) was −80 to −90 mV. Experiments were performed at room temperature. Currents were recorded with an Axopatch 200B amplifier (Molecular Devices), sampled at 20–50 kHz, low-pass filtered (eight-pole Bessel) at 5–10 kHz. Before analysis of P_o within a burst, data were digitally refiltered to give a cascaded low-pass filter cutoff frequency of 2 kHz. pClamp 9 or 10 (Molecular Devices) was used to acquire and analyse the data.

The principal goal of single-channel analysis was to measure the open probability (P_o) within bursts of channel openings, which provides a good estimate of P_o within an NMDAR activation[6,32,33]. To idealize single-channel data, transitions were detected by using a 50% threshold criterion[34]. Events of 200 μs duration or less were excluded from analysis. Missing and ignoring brief events can significantly influence dwell-time histograms. However, such brief events contribute only a tiny fraction of the total time that a channel spends open or closed. Thus, missed events should not have significantly affected measurements of P_o. Histograms are presented as square root versus log(time) plots[35]. Shut-time histograms were fitted with three or four exponential components. A burst was defined as a series of openings separated by closures of duration less than a critical duration, T_{crit}. Bursts with two levels of openings were discarded. We calculated T_{crit} between the two longest components of the shut-time histograms so that total number of event misclassifications was minimized[34,36]. For NR1wt/NR2Awt and NR1wt/NR2B-(2A NTD+L) receptors, the two longest components of the shut-time distribution differed by a mean factor of more than 390, whereas these components were less separated for NR1wt/NR2Bwt and NR1wt/NR2A-(2B NTD+L) (23-fold and 54-fold separation, respectively). For the latter two constructs, the separation between shut-time components results in a greater than desired number of misclassification of shut times[34]. This may have led to an overestimation of the P_o within a burst. However, for wild-type receptors, our data are consistent overall with previous results[6,33], suggesting that our estimates of P_o are reliable.

Chemicals. HEPES, L-glutamate, glycine, DTPA, EDTA, tricine and ADA were obtained from Sigma, D-APV from Ascent Scientific, 2-aminoethylmethanethiosulphonatehydrobromide (MTSEA), 2-(trimethylammonium)ethylmethanethiosulphonatebromide (MTSET) and 3-(triethylammonium)propylmethanethiosulphonatebromide (MTS-PtrEA) from Toronto Research Chemicals, and (+)-MK-801 from Tocris. MTS compounds were prepared as 40 mM stock solutions in doubly distilled water, aliquoted in small volumes (50 μl) and stored at −20 °C; aliquots were thawed just before use.

Construction of Fig. 4. The molecular architecture shown in Fig. 4a was illustrated by the crystal structure of the mGluR1 ligand-binding domain dimer (PDB 1ewv, ref. 37) at the level of the NTD, the NMDAR NR1/NR2A agonist-binding domain dimer (PDB 2a5T, ref. 30) and two subunits of the KcsA tetramer (PDB 1bl8, ref. 38) as the transmembrane region of the receptor. The third transmembrane segment and the C-terminal cytoplasmic region are lacking in this structural depiction.

31. Paoletti, P., Ascher, P. & Neyton, J. High-affinity zinc inhibition of NMDA NR1-NR2A receptors. *J. Neurosci.* **17,** 5711–5725 (1997).
32. Erreger, K. & Traynelis, S. F. Zinc inhibition of rat NR1/NR2A *N*-methyl-D-aspartate receptors. *J. Physiol. (Lond.)* **586,** 763–778 (2008).
33. Schorge, S., Elenes, S. & Colquhoun, D. Maximum likelihood fitting of single channel NMDA activity with a mechanism composed of independent dimers of subunits. *J. Physiol. (Lond.)* **569,** 395–418 (2005).
34. Colquhoun, D. & Sigworth, F. J. in *Single-channel Recording* (eds Sakmann, B. & Neher, E.) 483–587 (Plenum, 1995).
35. Sigworth, F. J. & Sine, S. M. Data transformations for improved display and fitting of single-channel dwell time histograms. *Biophys. J.* **52,** 1047–1054 (1987).
36. Jackson, M. B., Wong, B. S., Morris, C. E., Lecar, H. & Christian, C. N. Successive openings of the same acetylcholine receptor channel are correlated in open time. *Biophys. J.* **42,** 109–114 (1983).
37. Kunishima, N. *et al.* Structural basis of glutamate recognition by a dimeric metabotropic glutamate receptor. *Nature* **407,** 971–977 (2000).
38. Doyle, D. A. *et al.* The structure of the potassium channel: molecular basis of K^+ conduction and selectivity. *Science* **280,** 69–77 (1998).